

Experimental Evidence of Differences in the Hydrogen-Bonded Structure of Concentrated Aqueous Solutions Involving DL- and L-Alanine Molecules

Yasuo Kameda,* Motoya Sasaki, Masahiro Yaegashi, Yuko Amo, and Takeshi Usuki

Department of Material and Biological Chemistry, Faculty of Science, Yamagata University, Yamagata 990-8560

Received April 1, 2004; E-mail: kameda@sci.kj.yamagata-u.ac.jp

Time-of-Flight (TOF) and steady state reactor neutron diffraction measurements have been carried out for aqueous 2.5 mol% DL- and L-alanine solutions in order to investigate the differences in intermolecular hydrogen-bonded structure between solutions involving amino acid molecules with different optical activities. The observed difference functions, $\Delta i(Q)$ and $\Delta i^{\mathrm{inter}}(Q)$, between observed scattering cross sections for DL- and L-alanine solutions with a D content of 96.1% exhibit the first peak located at $Q = 2$ Å^{-1} followed by oscillatory features extending up to the higher-Q region. The difference distribution function, $\Delta g(r)$, obtained from the Fourier transform of $\Delta i(Q)$, clearly indicates negative peaks at $r = 2$ and 2.5 Å and a positive one at $r = 3.5$ Å. Partial structure factors, $a_{\mathrm{HH}}(Q)$, $a_{\mathrm{XH}}(Q)$, and $a_{\mathrm{XX}}(Q)$ (X: O, N, C, H_M, and H_M', where H_M and H_M' denote methyl and methine hydrogen atoms within the alanine molecule, respectively) for 2.5 mol% DL-alanine solutions are successfully determined from combined analyses of intermolecular interference terms observed for solutions with 96.1, 66.0, and 35.9% exchangeable deuterium content. The nearest neighbor O···H_{ex} and H_{ex}···H_{ex} (H_{ex}: exchangeable hydrogen atom) distances are determined from the least squares fit of the observed partial structure factors, 1.90(1) and 2.48(1) Å, respectively. These values correspond to the positions of negative peaks observed in the present $\Delta g(r)$ function. The least squares fitting analysis of the observed $\Delta i(Q)$ revealed that the difference in the coordination number of the nearest neighbor O···H_{ex} and H_{ex}···H_{ex} interactions between the DL- and L-alanine solutions are $-0.031(5)$ and $-0.072(5)$, respectively. It is concluded that the intermolecular hydrogen bonds among solvent water molecules in the DL-alanine solution are ca. 2% weaker than those in the L-alanine solution.

The optical activity of amino acid molecules plays an important role in various fields of chemistry and biology. Although the chemical properties of L-amino acids and the DL-racemic mixture (equimolar mixture of D- and L-amino acid molecules) are identical, the solubility in water is known to be slightly different between L- and DL-compounds.[1] This solubility difference is enhanced when the solvent is substituted by heavy water. In fact, the solubility of L-alanine in D_2O is ca. 17% lower than that for DL-alanine (3 mol% DL-alanine in the saturated solution).[2] This difference in solubility may be related to the different intermolecular hydrogen-bonded structure in the crystalline state.[3] On the other hand, this solubility difference may cause a difference in the hydrogen-bonded network of the solvent water molecules at higher solute concentrations. According to an earlier Monte Carlo simulation study on chiral discrimination between D- and L-alanine molecules, homochirality is slightly favorable at short intermolecular distances.[4] However, an experimental study on the effects of the different optical activity of solute molecules on the intermolecular hydrogen bonds among solvent molecules has not yet been reported. In order to deduce information on the intermolecular hydrogen bonds in solution, neutron diffraction with H/D isotopic substitution is one of the most suitable experimental techniques.

In the present paper, we describe the results of neutron diffraction measurements on aqueous 2.5 mol% DL- and L-alanine solutions with different H/D isotopic compositions in order to discuss the effects of differences in the optical activity of amino acid molecules on the intermolecular hydrogen-bonded structure in aqueous solution. The difference interference function, $\Delta i(Q)$, was determined from the difference between the scattering cross sections observed for DL- and L-alanine solutions in which 96.1% of the exchangeable hydrogen atoms have been substituted by deuterium atoms. The difference distribution function, $\Delta g(r)$, was obtained from the Fourier transform of the observed $\Delta i(Q)$. Intermolecular partial structure factors, $a_{\mathrm{HH}}(Q)$, $a_{\mathrm{XH}}(Q)$, and $a_{\mathrm{XX}}(Q)$, for the 2.5 mol% DL-alanine solution, were determined by a combined analysis of the intermolecular interference terms observed for solutions in which isotopic compositions of exchangeable hydrogen atoms were 96.1, 66.0, and 35.9% D.

Experimental

Materials. DL-$CH_3CH(NH_2)COOH$ and L-$CH_3CH(NH_2)$-$COOH$ (natural abundance, Nacalai Tesque, guaranteed grade) were dissolved in D_2O (99.9% D, Aldrich Chemical Co., Inc.) and in H_2O–D_2O mixtures to prepare six aqueous 2.5 mol% alanine solutions with different H/D isotopic ratios of exchangeable hydrogen atoms,

I: $[\mathrm{DL\text{-}CH_3CH(ND_2)COOD}]_{0.025}(D_2O)_{0.975}$,

II: $[\mathrm{L\text{-}CH_3CH(ND_2)COOD}]_{0.025}(D_2O)_{0.975}$,

III: $[\mathrm{DL\text{-}CH_3CH(N^0H_2)COO^0H}]_{0.025}(^0H_2O)_{0.975}$,

Published on the web October 9, 2004; DOI 10.1246/bcsj.77.1807

Table 1. Isotopic Composition and Average Scattering Length, $b_{H_{ex}}$, of Exchangeable Hydrogen Atom, Total Cross Sections and Number Density Scaled in the Stoichiometric Unit, $[CH_3CH(N^*H_2)COO^*H]_x(^*H_2O)_{1-x}$, σ_t and ρ, Respectively

Sample	H_{ex} /%	D_{ex} /%	$b_{H_{ex}}$ /10^{-12} cm	σ_t /barns[a)]	ρ /Å^{-3}
I [DL-$CH_3CH(ND_2)COOD]_{0.025}(D_2O)_{0.975}$ II [L-$CH_3CH(ND_2)COOD]_{0.025}(D_2O)_{0.975}$	3.9	96.1	0.626	19.700	
III [DL-$CH_3CH(N^0H_2)COO^0H]_{0.025}(^0H_2O)_{0.975}$[b)] IV [L-$CH_3CH(N^0H_2)COO^0H]_{0.025}(^0H_2O)_{0.975}$[b)]	64.1	35.9	0	57.074	0.03145
V [DL-$CH_3CH(N^{0-2}H_2)COO^{0-2}H]_{0.025}(^{0-2}H_2O)_{0.975}$[c)] VI [L-$CH_3CH(N^{0-2}H_2)COO^{0-2}H]_{0.025}(^{0-2}H_2O)_{0.975}$[c)]	34.0	66.0	0.313	37.131	

a) For incident neutron wavelength of 1.096 Å. b) The superscript "0" denotes the isotopic mixture in which the average coherent scattering length of exchangeable hydrogen atom is zero. c) The isotopic mixture with $b_{^{0-2}H} = (b_D + b_{^0H})/2$.

IV: [L-$CH_3CH(N^0H_2)COO^0H]_{0.025}(^0H_2O)_{0.975}$,
V: [DL-$CH_3CH(N^{0-2}H_2)COO^{0-2}H]_{0.025}(^{0-2}H_2O)_{0.975}$, and
VI: [L-$CH_3CH(N^{0-2}H_2)COO^{0-2}H]_{0.025}(^{0-2}H_2O)_{0.975}$,
respectively.

The superscript "0" in sample solutions III and IV denotes the null mixture, in which the average coherent scattering length of the exchangeable hydrogen atoms is set to zero. In sample solutions V and VI, the isotopic composition of the exchangeable hydrogen atoms has been chosen to be the mean value of D and ^{0}H, i.e., $b_{^{0-2}H} = (b_D + b_{^0H})/2$. The sample parameters used in the present study are listed in Table 1. The coherent scattering lengths, scattering and absorption cross sections for O, N, and C nuclei were those tabulated by Sears.[5] The wavelength dependence of the total cross sections for H and D nuclei was estimated from the observed total cross sections for liquid H_2O and D_2O, respectively.[6]

Reactor Based Neutron Diffraction Measurements. Sample solutions I to VI were sealed into cylindrical fused quartz cells (11.4 mm in inner diameter and 1.2 mm in thickness). Neutron diffraction measurements were carried out at 25 °C using the ISSP 4G (GPTAS) diffractometer installed at the JRR-3M research reactor operated at 20 MW in the Japan Atomic Energy Research Institute in Tokai, Japan. The incident neutron wavelength, $\lambda = 1.096 \pm 0.003$ Å, was determined from Bragg reflections from the KCl powder. Beam collimations used were 40′–80′–80′ in going from the reactor to the detector. The aperture of the collimated beam was 20 mm in width and 40 mm in height. Scattered neutrons were collected over the angular range of $3 \leq 2\theta \leq 115°$, corresponding to the scattering vector magnitude range of $0.30 \leq Q \leq 9.67$ Å^{-1} ($Q = 4\pi \sin\theta/\lambda$). The step interval was chosen to be $\Delta(2\theta) = 0.5°$ in the range of $3 \leq 2\theta \leq 40°$, and $\Delta(2\theta) = 1°$ in the range of $41 \leq 2\theta \leq 115°$, respectively. The preset neutron monitor count was 1160×10^6. Measurements of the scattering intensities from the vanadium rod (8 mm in diameter), empty cell, and background were made in advance. The total number of scattering neutrons accumulated for each data point of a sample solutions was at least 4.0×10^5, which corresponds to a statistical uncertainty of 0.16%.

TOF Neutron Diffraction Measurements. Sample solutions I and II were sealed into cylindrical Ti–Zr null alloy cells (8.0 mm in inner diameter and 0.3 mm in thickness). TOF neutron diffraction measurements were carried out at 25 °C using the HIT-II spectrometer[7] installed at the High Energy Accelerator Organization (KEK), Tsukuba, Japan. Scattered neutrons were detected by 104 ^{3}He counters covering a scattering angle of $10 \leq 2\theta \leq 157°$. The data accumulation time was ca. 8 h for each sample solution. Measurements were made in advance for an empty cell, instrumental background, and a vanadium rod of 8 mm in diameter.

Data Reduction. Reactor Data: The observed scattering intensities were corrected for background scattering and absorption by both the sample and cell.[8] The corrected count rate of the sample solution was converted to the absolute scale by the use of scattering intensities from the vanadium rod corrected for the absorption and the multiple scattering[9] contributions. The self scattering intensities for the sample solutions, which involve contributions from the coherent, incoherent, multiple, and inelasticity scattering, were estimated by the polynomial expansion method proposed by Bellissent-Funel et al.[10] The observed total scattering intensities, $(d\sigma/d\Omega)^{obs}$, involving coherent, incoherent, and multiple scattering contributions can be approximated by the following equation:

$$(d\sigma/d\Omega)^{obs} = \alpha[(d\sigma/d\Omega)_{int}{}^{intra} + (d\sigma/d\Omega)_{int}{}^{inter} + (d\sigma/d\Omega)^{self}], \quad (1)$$

where α denotes the normalization factor, in which the uncertainty in the absorption correction is included. $(d\sigma/d\Omega)_{int}{}^{intra}$ and $(d\sigma/d\Omega)_{int}{}^{inter}$ stand for the intra- and intermolecular interference terms. $(d\sigma/d\Omega)_{int}{}^{intra}$ scaled in the stoichiometric units, $[CH_3CH(N^*H_2)COO^*H]_x(^*H_2O)_{1-x}$, is represented by the sum of contributions from alanine and water molecules, i.e.,

$$(d\sigma/d\Omega)_{int}{}^{intra} = x(d\sigma/d\Omega)_{int}{}^{intra}(\text{for alanine}) + (1-x)(d\sigma/d\Omega)_{int}{}^{intra}(\text{for } ^*H_2O), \quad (2)$$

where

$$(d\sigma/d\Omega)_{int}{}^{intra}(\text{for alanine}) = \sum_{i\neq j}\sum b_i b_j \exp(-l_{ij}{}^2Q^2/2)\sin(Qr_{ij})/(Qr_{ij}), \quad (3)$$

and

$$(d\sigma/d\Omega)_{int}{}^{intra}(\text{for } ^*H_2O) = 4b_O b_H \exp(-l_{OH}{}^2Q^2/2)\sin(Qr_{OH})/(Qr_{OH}) + 2b_H{}^2 \exp(-l_{HH}{}^2Q^2/2)\sin(Qr_{HH})/(Qr_{HH}), \quad (4)$$

Parameters, l_{ij} and r_{ij}, denote the root mean square displacement and internuclear distance for the i–j pair. Values of r_{ij} and l_{ij} for the alanine molecule used for Eq. 3 were taken from the literature, which were determined from single crystal X-ray diffraction[3,11,12] and from gas phase electron diffraction[13] studies, respectively. In-

tramolecular parameters for the water molecule, r_{OH}, r_{HH}, l_{OH}, and l_{HH}, were those determined from neutron diffraction studies for liquid pure water.[14,15] The self term in Eq. 1 can be expanded in the following polynomial function of Q:

$$(d\sigma/d\Omega)^{self} = (d\sigma/d\Omega)^{coh} + (d\sigma/d\Omega)^{inc} + (d\sigma/d\Omega)^{multi} = A + BQ^2 + CQ^4 + DQ^6 + EQ^8. \quad (5)$$

Coefficients A–E in Eq. 5 and the normalization factor α in Eq. 1 were determined by a least squares fit to the observed total scattering cross section in the range of $3.00 \leq Q \leq 9.67$ Å^{-1}. The fitting procedure was performed by the SALS program.[16]

The intermolecular interference term, $(d\sigma/d\Omega)_{int}^{inter}$, was evaluated by the following equation:

$$(d\sigma/d\Omega)_{int}^{inter} = (d\sigma/d\Omega)^{obs}/\alpha - (d\sigma/d\Omega)_{int}^{intra} - (d\sigma/d\Omega)^{self}. \quad (6)$$

The intermolecular difference function, $\Delta i^{inter}(Q)$, between the DL- and L-alanine solutions was obtained from the following equation:

$$\Delta i^{inter}(Q) = (d\sigma/d\Omega)_{int}^{inter}(\text{for DL-alanine solution}) - (d\sigma/d\Omega)_{int}^{inter}(\text{for L-alanine solution}). \quad (7)$$

The intermolecular difference distribution function, $\Delta g^{inter}(r)$, was determined by the Fourier transform of the $\Delta i^{inter}(Q)$:

$$\Delta g^{inter}(r) = (2\pi\rho r^2)^{-1} \int_0^{Q_{max}} Q\Delta i^{inter}(Q) \sin(Qr)dQ. \quad (8)$$

The upper limit of the integral, Q_{max}, was chosen to be 9.6 Å^{-1}.

Intermolecular partial structure factors for the DL-alanine solution, $a_{HH}(Q)$, $a_{XH}(Q)$, and $a_{XX}(Q)$ (X; O, N, C, H_M, and H_M'), were deduced from the combination of observed $(d\sigma/d\Omega)_{int}^{inter}$ terms for three sample solutions, I, III, and V, which are all identical except for the H/D isotopic ratio of the exchangeable hydrogen atom:

$$\begin{aligned}&(d\sigma/d\Omega)_{int}^{inter}(\text{for I}) + (d\sigma/d\Omega)_{int}^{inter}(\text{for III}) - 2(d\sigma/d\Omega)_{int}^{inter}(\text{for V})\\ &= (2+x)^2/2b_D^2[a_{HH}(Q) - 1]\\ &= 0.8035[a_{HH}(Q) - 1], \end{aligned} \quad (9)$$

$$\begin{aligned}&4(d\sigma/d\Omega)_{int}^{inter}(\text{for V}) - (d\sigma/d\Omega)_{int}^{inter}(\text{for I}) - 3(d\sigma/d\Omega)_{int}^{inter}(\text{for III})\\ &= 2[(1+x)b_O + xb_N + 3xb_C + 3xb_{H_M} + xb_{H_M'}](2+x)b_D[a_{XH}(Q) - 1]\\ &= 1.5991[a_{XH}(Q) - 1], \end{aligned} \quad (10)$$

and

$$\begin{aligned}&(d\sigma/d\Omega)_{int}^{inter}(\text{for III})\\ &= [x(b_N + 3b_C + 3b_{H_M} + b_{H_M'}) + (1+x)b_O]^2[a_{XX}(Q) - 1]\\ &= 0.3977[a_{XX}(Q) - 1], \end{aligned} \quad (11)$$

where x denotes the mole fraction of the alanine molecule. The present $a_{XH}(Q)$ is represented as a linear combination of partial structure factors concerning O–H_{ex}, N–H_{ex}, C–H_{ex}, H_M–H_{ex}, and H_M'–H_{ex} pairs. Since the contribution from the O–H_{ex} partial structure factor occupies 94% of the total in the present experiment, the observed $a_{XH}(Q)$ is considered to represent intermolecular hydrogen-bonded structure among solvent water molecules. The contribution of the O–O partial structure factor amounts to 89% of the observed $a_{XX}(Q)$. The present $a_{XX}(Q)$ can be approximated as the O–O partial structure factor.

The intermolecular distance, root mean square displacement, and coordination number, r_{ij}, l_{ij}, and n_{ij}, for the i–j atom pair, were determined by a least squares fit of the observed intermolecular partial structure factors to the corresponding calculated ones, $a_{ij}^{calc}(Q)$, which involve the contribution from the long-range random distribution of atoms as follows:[17–19]

$$\begin{aligned}a_{ij}^{calc}(Q) = &\sum \beta_{ij} n_{ij} \exp(-l_{ij}^2Q^2/2)\sin(Qr_{ij})/(Qr_{ij})\\ &+ 4\pi\rho\exp(-l_0^2Q^2/2)[Qr_0\cos(Qr_0)\\ &- \sin(Qr_0)]Q^{-3}, \end{aligned} \quad (12)$$

where ρ gives the number density of the stoichiometric unit $[CH_3CH(N^*H_2)CO^*OH]_x(^*H_2O)_{1-x}$. The parameter r_0 denotes the distance beyond which the uniform distribution is assumed, and l_0 describes the sharpness of the boundary at r_0. The coefficient β_{ij} in Eq. 12 is given as

$$\beta_{HH} = (2+x)^{-1}, \quad (13)$$

and

$$\beta_{XH} = \gamma_{XH}[(2+x)\{[(1+x)b_O + x(b_N + 3b_C + 3b_{H_M} + b_{H_M'})]\}^{-1}, \quad (14)$$

where $\gamma_{OH} = (1+x)b_O$ and

$$\beta_{XX} = \delta_{XX}[x(b_N + 3b_C + 3b_{H_M} + b_{H_M'}) + (1+x)b_O]^{-2}. \quad (15)$$

Here, $\delta_{OO} = (1+x)b_O^2$ and $\delta_{NO} = xb_N^2$. The fitting procedure was performed in the range of $0.5 \leq Q \leq 9.6$ Å^{-1} using the SALS program.[16]

The partial distribution function, $g_{ij}(r)$, is derived from the Fourier transform of the observed $a_{ij}(Q)$:

$$g_{ij}(r) = 1 + (2\pi\rho r^2)^{-1} \int_0^{Q_{max}} Q[a_{ij}(Q) - 1]\sin(Qr)dQ. \quad (16)$$

The upper limit of the integral was taken to be $Q_{max} = 9.6$ Å^{-1}.

TOF Neutron Diffraction Data: The observed scattering intensities corrected for the instrumental background, absorption of both the sample and cell,[8] were converted to the absolute scale by the use of corrected scattering intensities from the vanadium rod. The difference function, $\Delta i(Q)$, between the scattering cross sections observed for DL- and L-alanine solutions in D_2O is:

$$\Delta i(Q) = (d\sigma/d\Omega)^{obs}(\text{for DL-alanine solution}) - (d\sigma/d\Omega)^{obs}(\text{for L-alanine solution}). \quad (17)$$

The intramolecular interference term and the inelasticity contribution arising from the H and D nuclei is expected to cancel out in the present $\Delta i(Q)$ function. Since the $\Delta i(Q)$ from the 64 sets of forward angle detectors located at $10 \leq 2\theta \leq 51^\circ$ agree well within the statistical uncertainties, they were combined at the Q-interval of 0.1 Å^{-1}, and employed for the subsequent analysis. The difference distribution function, $\Delta g(r)$, was evaluated by the Fourier transform,

$$\Delta g(r) = (2\pi\rho r^2)^{-1} \int_0^{Q_{max}} Q\Delta i(Q)\sin(Qr)dQ. \quad (18)$$

The upper limit of the integral was set to $Q_{max} = 20$ Å^{-1}. The

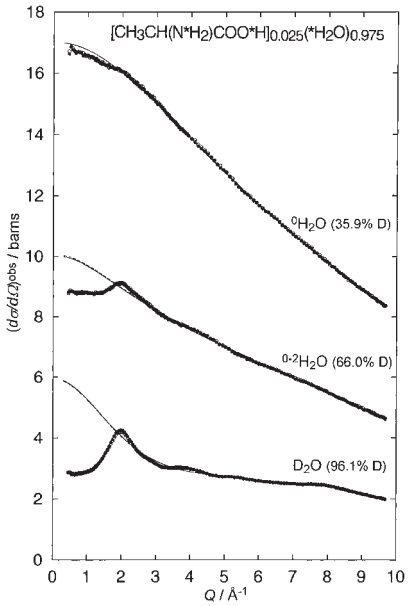

Fig. 1. Observed scattering cross sections, $(d\sigma/d\Omega)^{obs}$, for aqueous 2.5 mol% DL-alanine (full circles) and L-alanine (open circles) solutions with different H/D ratios of exchangeable hydrogen atoms. Solid and broken lines denote the self scattering term in Eq. 5 for DL- and L-alanine solutions, respectively.

$\Delta g(r)$ function truncated at $Q_{max} = 9.6$ Å^{-1} was also evaluated for purposes of comparison with the reactor data. Since the sum of contributions from the O–H_{ex} and H_{ex}–H_{ex} partial structure factors corresponds to 86% of the observed total interference term in the present experimental conditions, the present $\Delta g(r)$ reflects the difference in the intermolecular hydrogen-bonded structure between the DL- and L-alanine solutions.

Results and Discussion

Scattering cross sections for sample solutions I–VI observed from the reactor measurements are represented in Fig. 1. The values of $(d\sigma/d\Omega)^{obs}$ for the DL- and L-alanine solutions with the same H/D ratio look very similar, however, an indication of the systematic difference can be observed in the region of the first diffraction peak at $Q \approx 2$ Å^{-1} between the solutions containing 96.1% D, which will be discussed later. A gradual decrease in the intensity of $(d\sigma/d\Omega)^{obs}$ in the larger-Q region is mainly due to the inelasticity effect of the H atom in the solution, which becomes more pronounced for solutions with higher-H content.

Figure 2 shows the difference, $\delta(Q)$, between scattering cross sections observed for DL- and L-alanine solutions which have the same H/D ratio. The $\delta(Q)$ function for the ^0H_2O and $^{0-2}H_2O$ solutions exhibits no systematic structure within the statistical uncertainties. However, interference features can be obviously identified in the $\delta(Q)$ for the D_2O (96.1% D) solutions. This result implies that there is some difference in the solution structure between DL- and L-alanine heavy water solutions at this solute concentration. In order to deduce quantitative information on the structural difference between the DL- and L-alanine heavy water solutions, the difference function, $\Delta i^{inter}(Q)$, between the renormalized intermolecular

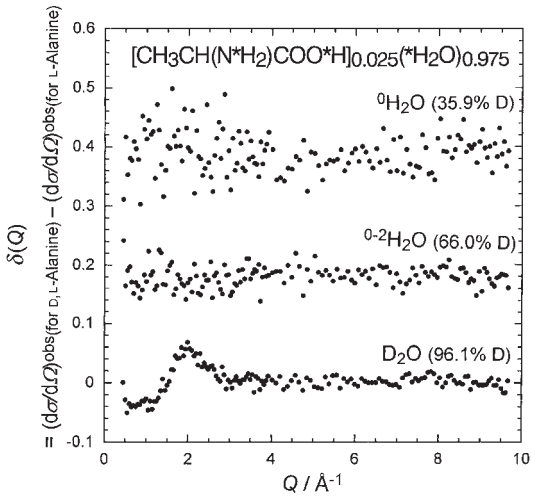

Fig. 2. Observed difference function, $\delta(Q)$, between scattering cross sections for aqueous 2.5 mol% DL- and L-alanine solutions with different H/D ratios of exchangeable hydrogen atoms.

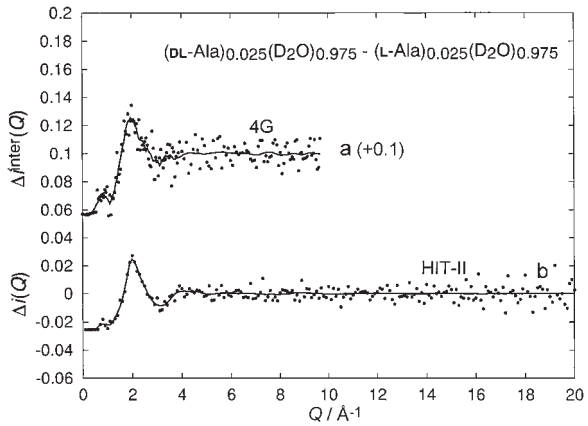

Fig. 3. a) Dots: The intermolecular difference function, $\Delta i^{inter}(Q)$, obtained from the reactor experiment. Solid line: Smoothed $\Delta i^{inter}(Q)$ used for the Fourier transform. b) Dots: The total difference function, $\Delta i(Q)$, observed by the TOF experiment. Solid line: The smoothed $\Delta i(Q)$ used for the Fourier transform.

interference term $(d\sigma/d\Omega)_{int}^{inter}$ for sample solutions I and II has been obtained, as shown in Fig. 3a. Although the data points are somewhat scattered due to statistical uncertainties, a diffraction peak at $Q \approx 2$ Å^{-1} is clearly observed. The difference function, $\Delta i(Q)$, deduced from the TOF measurement is represented in Fig. 3b. The interference features in $\Delta i(Q)$ are in good agreement with those observed in the $\Delta i^{inter}(Q)$ from the reactor data within the statistical uncertainties, indicating that the present difference functions, $\Delta i^{inter}(Q)$ and $\Delta i(Q)$, are reliable, and features appearing in the difference functions can be considered to be real.

Figure 4a shows the observed difference distribution function, $\Delta g^{inter}(r)$, which reflects the structural difference in intermolecular hydrogen bonds between the DL- and L-alanine solutions. The present $\Delta g^{inter}(r)$ is characterized by a negative peak at around $r = 2$ Å, implying that the intermolecular interaction

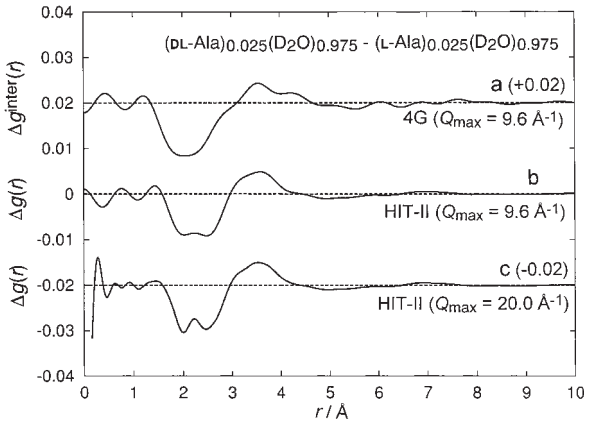

Fig. 4. a) The intermolecular difference distribution function, $\Delta g^{\mathrm{inter}}(r)$, observed by the reactor experiment. The upper limit of the Fourier transform is set to be $Q_{\max} = 9.6$ Å^{-1}. b) The total difference distribution function, $\Delta g(r)$, observed by the TOF experiment. The upper limit of the Fourier transform is set to be $Q_{\max} = 9.6$ Å^{-1}. c) The same notations as in b) except for $Q_{\max} = 20$ Å^{-1}.

is less pronounced in this region in the DL-alanine solution than that in the L-alanine solution. An asymmetric shape of this negative peak may suggest that the peak involves several interatomic interactions. In the present $\Delta g^{\mathrm{inter}}(r)$, a positive peak is observed in the region of $r = 3$–4 Å. Figure 4b shows the $\Delta g(r)$ obtained from the TOF measurement, which has been truncated at the same upper limit as that employed for the reactor data, $Q_{\max} = 9.6$ Å^{-1}. Structural features appearing in $\Delta g(r)$ are very similar to those observed in the $\Delta g^{\mathrm{inter}}(r)$, again indicating that the structural difference between the DL- and L-alanine solutions certainly exists. The negative feature around $r \approx 2$ Å is resolved into partially resolved peaks located at $r \approx 2$ and 2.5 Å in $\Delta g(r)$ truncated at $Q_{\max} = 20$ Å^{-1} (Fig. 4c). Positions of these peaks correspond well to those for the nearest neighbor O···H and H···H hydrogen-bonded interactions reported for pure liquid water[20–23] and for aqueous NH_4Cl[24] and LiBr[25] solutions.

In order to obtain detailed structural information concerning the intermolecular structure among solvent water molecules in the present solution, the partial structure factors $a_{\mathrm{HH}}(Q)$, $a_{\mathrm{XH}}(Q)$, and $a_{\mathrm{XX}}(Q)$ for the 2.5 mol% DL-alanine solution were derived from the intermolecular interference terms for samples I, III, and V observed in the reactor experiments. Since it is possible that the intermolecular structure in the present solution depends slightly on the H/D ratio of exchangeable hydrogen atoms, the present partial structure factors are regarded as approximated ones. It might be possible to deduce the partial structure factors for the L-alanine solution, however, the H/D ratio dependence on the intermolecular structure may be more pronounced for the L-alanine solution considering the larger difference in the solubility of the L-alanine for H_2O and D_2O,[2] as mentioned in the introduction section. Partial structure factors derived from the observed scattering intensities for DL-alanine solutions are therefore considered to be more reliable.

Figure 5 shows the partial structure factors observed for the

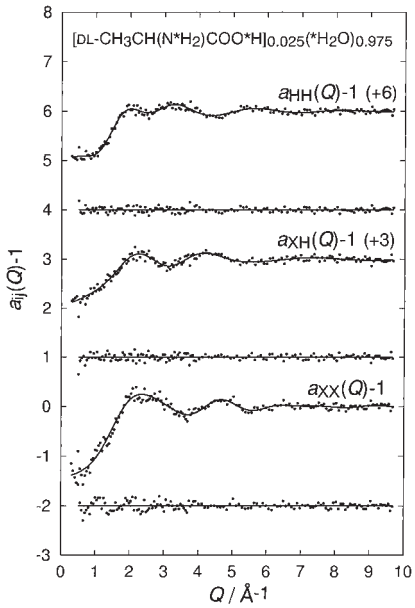

Fig. 5. Circles: Observed H–H, X–H, and X–X partial structure factors, $a_{\mathrm{ij}}(Q)$, for aqueous 2.5 mol% DL-alanine solutions. Solid lines: The best-fit of calculated interference terms in Eq. 12. The difference between observed and calculated $a_{\mathrm{ij}}(Q)$ is shown below.

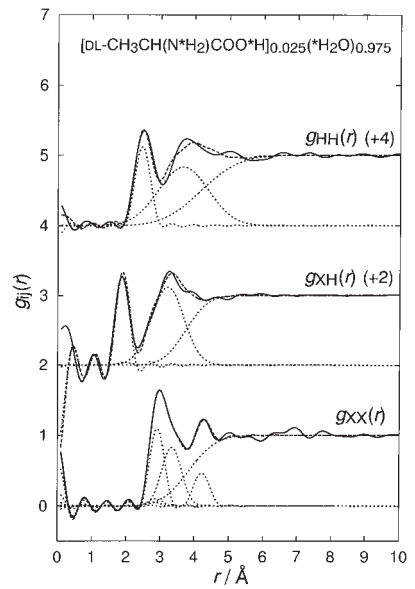

Fig. 6. Solid line: Observed H–H, X–H, and X–X partial distribution functions, $g_{\mathrm{ij}}(r)$, for aqueous 2.5 mol% DL-alanine solutions. Broken lines: The Fourier transform of the solid lines in Fig. 5. Contributions from the short- and long-range interactions are denoted by dotted lines.

2.5 mol% DL-alanine solution. Interference features can be obviously identified in the present $a_{\mathrm{ij}}(Q)$ functions. The intermolecular partial distribution functions $g_{\mathrm{HH}}(r)$, $g_{\mathrm{XH}}(r)$, and $g_{\mathrm{XX}}(r)$ are represented in Fig. 6. The nearest neighbor H_{ex}···H_{ex} and O···H_{ex} interactions are observed as the resolved first peaks at $r = 2.5$ and 1.9 Å in the present $g_{\mathrm{HH}}(r)$ and $g_{\mathrm{XH}}(r)$ functions, respectively. The first peak in the $g_{\mathrm{XX}}(r)$ is attributable to the nearest neighbor O···O interaction. Structural parameters

on intermolecular interactions were determined through a least squares fit of the observed $a_{ij}(Q)$ applying the model function (Eq. 12) involving both short- and long-range interactions. Prior to the fitting analysis, the correction for low-frequency systematic errors in the observed $a_{ij}(Q)$ was applied.[15] The least squares refinement was performed in the range of $0.5 \leq Q \leq 9.6$ Å^{-1} using the SALS program,[16] assuming that statistical uncertainties distribute uniformly. In the fitting procedure for the observed $a_{HH}(Q)$ and $a_{XH}(Q)$, the number of short-range interactions was assumed to be two, while at least three short-range O···O interactions were found to be necessary to reproduce both the $a_{XX}(Q)$ and $g_{XX}(r)$ functions. In the fitting of the present $a_{XX}(Q)$, the nearest neighbor N(alanine)···O(water) and O(carboxyl)···O(water) interactions were taken into account with fixed structural parameters, which had been reported for the 3 mol% DL-alanine heavy water solution ($r_{NO} = 2.88$ Å, $l_{NO} = 0.18$ Å, and $n_{NO} = 2.40$)[26] and reported for the 8 mol% CH_3COONa solution ($r_{OO} = 2.78$ Å, $l_{OO} = 0.21$ Å, and $n_{OO} = 2.0$),[27] respectively.

Results of the least squares fit for the observed $a_{ij}(Q)$s are represented in Fig. 5. A satisfactory agreement is obtained between the observed and calculated $a_{ij}(Q)$ over the whole Q-range employed. The final values of all independent parameters are summarized in Table 2. The present value of the nearest neighbor O···H_{ex} distance, 1.90(1) Å, is in good agreement with that reported for pure liquid water ($r_{OH} = 1.85$ Å)[20,22] and those reported for aqueous 8 mol% NH_4Cl ($r_{OH} = 1.91$ Å)[24] and 10 mol% LiBr ($r_{OH} = 1.91$ Å)[25] solutions. The coordination number, n_{OH}, for the nearest neighbor O···H_{ex} interaction was determined to be 1.64(2). The nearest neighbor H_{ex}···H_{ex} and O···O distances were obtained to be 2.48(1) and 2.93(2) Å, respectively. These results suggest that the hydrogen-bonded network among the solvent water molecules is well maintained in the present 2.5 mol% DL-alanine solution. Additionally, it was revealed that the first negative peak observed in the difference distribution function $\Delta g(r)$ is attributable to the sum of contributions from intermolecular O···H_{ex} and H_{ex}···H_{ex} interactions.

Table 2. Results of the Least-Square Refinement for Partial Structure Factors, $a_{HH}(Q)$, $a_{XH}(Q)$, and $a_{XX}(Q)$, Observed for Aqueous 2.5 mol% DL-Alanine Solutions[a)]

		$a_{HH}(Q)-1$	$a_{XH}(Q)-1$	$a_{XX}(Q)-1$
1st nearest neighbor	i–j	H_{ex}–H_{ex}	O–H_{ex}	O–O
	r_{ij}/Å	2.48(1)	1.90(1)	2.93(2)
	l_{ij}/Å	0.20(1)	0.15(1)	0.19(1)
	n_{ij}	2.92(3)	1.64(2)	2.3(5)
2nd nearest neighbor	i–j	H_{ex}–H_{ex}	O–H_{ex}	N–O[b)]
	r_{ij}/Å	3.80(2)	3.28(1)	2.88(fixed)
	l_{ij}/Å	0.71(1)	0.47(1)	0.18(fixed)
	n_{ij}	17 (2)	11.9 (4)	2.40(fixed)
3rd nearest neighbor	i–j	—	—	O_C–O[c)]
	r_{ij}/Å	—	—	2.78(fixed)
	l_{ij}/Å	—	—	0.21(fixed)
	n_{ij}	—	—	2.0(fixed)
4th nearest neighbor	i–j		—	O–O
	r_{ij}/Å	—	—	3.36(5)
	l_{ij}/Å	—	—	0.29(5)
	n_{ij}	—	—	3.3(5)
5th nearest neighbor	i–j	—	—	O–O
	r_{ij}/Å	—	—	4.24(1)
	l_{ij}/Å	—	—	0.21(1)
	n_{ij}	—	—	2.23(1)
Long-range interaction	r_0/Å	4.3(1)	3.80(3)	3.94(1)
	l_0/Å	0.86(8)	0.52(3)	0.63(1)

a) Estimated standard deviations are given in parentheses. b) Fixed at values reported for 3 mol% DL-alanine heavy water solutions.[26] c) Fixed at values reported for aqueous 8 mol% CH_3COONa solutions.[27]

In order to obtain quantitative information on the present $\Delta i(Q)$ observed from the TOF neutron diffraction measurement, a least squares fitting analysis was adopted. In the refinement procedure, the following model function was employed:

$$\Delta i^{\mathrm{model}}(Q) = \sum (2-\delta_{ij}) c_i \Delta n_{ij} b_i b_j \times \exp(-l_{ij}^2 Q^2/2) \sin(Q r_{ij})/(Q r_{ij}), \quad (19)$$

where $\delta_{ij} = 1$, (i = j) and $\delta_{ij} = 0$, (i ≠ j). c_i denotes the number of atoms i in the stoichiometric unit, $[CH_3CH(N^*H_2)COO^*H]_x(^*H_2O)_{1-x}$. Δn_{ij} stands for the difference in the coordination number between the DL- and L-alanine solutions. Parameters Δn_{ij}, l_{ij}, and r_{ij}, were determined by the least squares fit of Eq. 19 to the observed $\Delta i(Q)$. The fitting was performed in the range of $2.5 \leq Q \leq 15$ Å^{-1} using the SALS program.[16] Parameters for the nearest neighbor O···H_{ex} and H_{ex}···H_{ex} interactions were refined independently. The positive peak appearing at $r \sim 3.5$ Å was assumed to be a single interaction in order to reduce the number of independent parameters and also to improve the fit in the lower-Q region.

The $\Delta i^{\mathrm{model}}(Q)$ calculated from the best-fit model was compared with the observed $\Delta i(Q)$ in Fig. 7. A satisfactory agreement is obtained between the observed and calculated difference functions. The corresponding distribution function $\Delta g(r)$ is represented in Fig. 8. The final values of all independent parameters are summarized in Table 3. The values of the nearest neighbor intermolecular O···H_{ex} and H_{ex}···H_{ex} distances

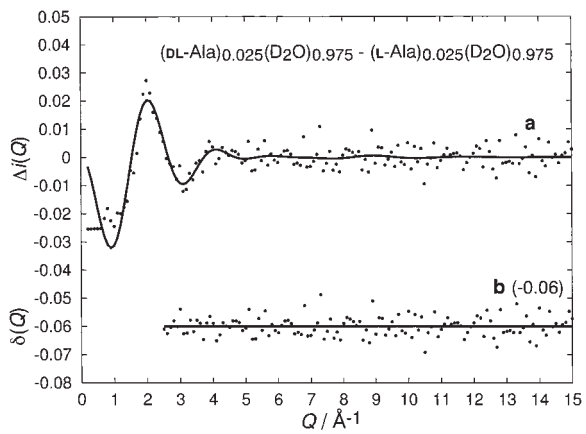

Fig. 7. a) Circles: Observed difference interference function, $\Delta i(Q)$, between the DL- and L-alanine solutions. Solid line: The best-fit of the calculated interference term in Eq. 19. b) The difference between observed and calculated $\Delta i(Q)$.

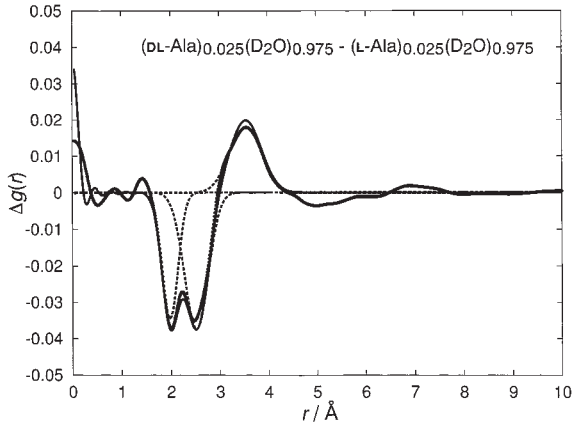

Fig. 8. Circles: Observed difference distribution function, $\Delta g(r)$, truncated at $Q_{max} = 20$ Å^{-1}. Solid line: The Fourier transform of the solid line in Fig. 7a. Contributions from the short-range interactions are denoted by broken lines.

Table 3. Results of the Least-Square Refinement for the Difference Interference Function, $\Delta i(Q)$, between 2.5 mol% DL- and L-Alanine Solutions[a)]

i···j	r_{ij}/Å	l_{ij}/Å	Δn_{ij}
O···H_{ex}(I)	1.99(3)	0.170(8)	−0.031(5)
H_{ex}···H_{ex}	2.54(2)	0.23(5)	−0.072(5)
O···H_{ex}(II)[b)]	3.57(1)	0.32(2)	0.052(4)

a) Estimated standard deviations are given in parentheses. b) Involving contributions from O···H_{ex}, H_{ex}···H_{ex}, and O···O interactions.

were slightly larger than those determined from the partial structure factors for the DL-alanine solution, which have been discussed above. This suggests that the average intermolecular hydrogen bonded O···H_{ex} and H_{ex}···H_{ex} distances in the L-alanine solution might be slightly longer than those in the DL-alanine solution. The values of the root-mean-square displacements for intermolecular O···H_{ex} and H_{ex}···H_{ex} interactions determined from the $\Delta i(Q)$ are in good agreement with those obtained from the partial structure factors $a_{HX}(Q)$ and $a_{HH}(Q)$. The difference in the coordination number for the nearest neighbor intermolecular O···H_{ex} interaction $\Delta n_{OH_{ex}}$ was obtained to be −0.031(5), which corresponds to 1.9% of the value of $n_{OH_{ex}} = 1.64(2)$ obtained for the DL-alanine solution. The magnitude of the present $\Delta n_{H_{ex}H_{ex}}$ (= −0.072(5)) is 2.5% of the coordination number for the nearest neighbor H_{ex}···H_{ex} interaction. These results suggest that the intermolecular hydrogen bonds in the L-alanine solution are ca. 2% stronger than those in the DL-alanine solution.

In conclusion, experimental evidence has elucidated the difference in the intermolecular hydrogen-bonded structure between aqueous solutions involving DL- and L-alanine molecules. The difference in the coordination number of the nearest neighbor hydrogen-bonded O···H_{ex} and H_{ex}···H_{ex} interactions is estimated to be ca. 2%. The present results indicate that the difference in the optical activity of the solute molecules actually affects the hydrogen-bonded network in the aqueous solution.

The authors would like to acknowledge Prof. Hideki Yoshizawa (ISSP, University of Tokyo) and Mr. Yoshihisa Kawamura (ISSP, University of Tokyo) for their help during the course of the neutron diffraction measurements by the 4G diffractometer. We are indebted to Prof. Toshiharu Fukunaga (Kyoto University) and Dr. Keiji Itoh (Kyoto University) for their help with the TOF neutron diffraction measurements using the HIT-II spectrometer. All calculations were performed using the PRIMEPOWER 800 computer at the Yamagata University Computing Service Center. This work was partially supported by Grant-in-Aid for Scientific Research Nos. 1604125 and 16550049 from the Ministry of Education, Culture, Sports, Science and Technology.

References

1 "Kagaku Binran," Maruzen Co. Ltd. (1993), p. II-176.
2 Y. Kameda and M. Yaegashi, unpublished data (2002).
3 H. J. Simpson, Jr. and R. E. Marsh, *Acta Crystallogr.*, **20**, 550 (1966).
4 D. Andelman and H. Orland, *J. Am. Chem. Soc.*, **115**, 12322 (1993).
5 V. F. Sears, *Neutron News*, **3**, 26 (1992).
6 J. R. Granada, V. H. Gillete, and R. E. Mayer, *Phys. Rev. A*, **36**, 5594 (1987).
7 T. Fukunaga, M. Misawa, I. Fujikura, and S. Satoh, "KENS REPOR-IX" (1993), p. 16.
8 H. H. Paalman and C. J. Pings, *J. Appl. Phys.*, **33**, 2635 (1962).
9 I. A. Blech and B. L. Averbach, *Phys. Rev.*, **137**, A1113 (1965).
10 M.-C. Bellissent-Funel, L. Bisio, and J. Texeira, *J. Phys.: Condens Matter*, **3**, 4065 (1991).
11 J. D. Dunitz and R. R. Ryan, *Acta Crystallogr.*, **21**, 617 (1966).
12 M. Subha Nardhini, R. V. Krishnakumar, and S. Natarajan, *Acta Crystallogr.*, **C57**, 614 (2001).
13 K. Iijima and B. Beagley, *J. Mol. Struct.*, **248**, 133 (1991).
14 J. G. Powles, *Mol. Phys.*, **42**, 757 (1981).
15 Y. Kameda and O. Uemura, *Bull. Chem. Soc. Jpn.*, **65**, 2021 (1992).
16 T. Nakagawa and Y. Oyanagi, "Recent Development in Statistical Inference and Data Analysis," ed by K. Matushita, North-Holland (1980), p. 221.
17 A. H. Narten, M. D. Danford, and H. A. Levy, *Discuss. Faraday Trans.*, **43**, 97 (1967).
18 R. Caminiti, P. Cucca, M. Monduzzi, G. Saba, and G. Crisponi, *J. Chem. Phys.*, **81**, 543 (1984).
19 H. Ohtaki and N. Fukushima, *J. Solution Chem.*, **21**, 23 (1992).
20 A. K. Soper and M. G. Phillips, *Chem. Phys.*, **107**, 47 (1986).
21 P. Postrino, M. A. Ricci, and A. K. Soper, *J. Chem. Phys.*, **101**, 4123 (1994).
22 A. K. Soper, F. Bruni, and M. A. Ricci, *J. Chem. Phys.*, **106**, 247 (1997).
23 Y. Kameda, T. Usuki, and O. Uemura, *Bull. Chem. Soc. Jpn.*, **71**, 1305 (1998).
24 Y. Kameda, K. Sugawara, T. Usuki, and O. Uemura, *J. Phys. Soc. Jpn.*, **70**, Suppl. A, 362 (2001).
25 Y. Kameda, M. Imano, M. Takeuchi, S. Suzuki, T. Usuki,

and O. Uemura, *J. Non-Cryst. Solids*, **293–295**, 600 (2001).
26 Y. Kameda, K. Sugawara, T. Usuki, and O. Uemura, *Bull. Chem. Soc. Jpn.*, **76**, 935 (2003).
27 H. Naganuma, Y. Kameda, T. Usuki, and O. Uemura, *J. Phys. Soc. Jpn.*, **70**, Suppl. A, 356 (2001).